

NUMERICAL SIMULATION OF THE GENERALIZED BURGER'S-HUXLEY EQUATION VIA TWO MESHLESS METHODS

by

**Imtiaz AHMAD^{a*}, Sayed ABDEL-KHALEK^b,
Ahmed Mohammed ALGHAMDI^c, and Mustafa INC^{d,e*}**

^a Department of Mathematics, University of Swabi, Swabi, Khyber Pakhtunkhwa, Pakistan

^b Department of Mathematics, College of Science, Taif University, Taif, Saudi Arabia

^c Department of Software Engineering, College of Computer Science and Engineering,
University of Jeddah, Jeddah, Saudi Arabia

^d Firat University, Science Faculty, Department of Mathematics, Elazig, Turkiye

^e Department of Medical Research, China Medical University, Taichung, Taiwan

Original scientific paper

<https://doi.org/10.2298/TSCI22S1463A>

Numerical solution of the generalized Burger's-Huxley equation is established utilizing two effective meshless methods namely: local differential quadrature method and global method of line. Both the proposed meshless methods used radial basis functions to discretize space derivatives which convert the given model equation system of ODE and then we have utilized the Euler method to get the required numerical solution. Numerical experiments are carried out to check the efficiency and accuracy of the suggested meshless methods.

Key words: meshless differential quadrature method, meshless method of line, radial basis function, generalized Burger's-Huxley equation

Introduction

Non-linear partial differential equations (NLPDE) appear in diverse fields of science, mainly in engineering, physics, and chemistry. The NLPDE systems have become increasingly important in the research of evolutionary equations that describe wave propagation and in the investigation of the Brusselator chemical-diffusion reaction model. One of the most renowned NLPDE is the Burger's-Huxley equation. Satsuma [1] explored a generalised Burger's-Huxley equation:

$$\frac{\partial W(x,t)}{\partial t} + \alpha W(x,t)^\xi \frac{\partial W(x,t)}{\partial x} - \frac{\partial^2 W(x,t)}{\partial x^2} - \beta W(x,t)(1-W(x,t)^\xi)(W(x,t)^\xi - \eta) = 0 \quad (1)$$
$$x \in \Omega \subset \mathbb{R}, t \geq 0$$

with the conditions:

$$W(x,0) = \left[\frac{\eta}{2} + \frac{\eta}{2} \tanh(\omega_1 x) \right]^{1/\xi} \quad (2)$$

$$W(x,t) = \left\{ \frac{\eta}{2} + \frac{\eta}{2} \tanh[\omega_1(x - \omega_2 t)] \right\}^{1/\xi}, \quad x \in \partial\Omega, t > 0 \quad (3)$$

* Corresponding author, e-mails: imtiazkakahil@gmail.com, minc@firat.edu.tr

The exact solution [2]:

$$W(x, t) = \left\{ \frac{\eta}{2} + \frac{\eta}{2} \tanh[\omega_1(x - \omega_2 t)] \right\}^{1/\xi}, \quad x \in \Omega \subset \mathbb{R}, t \geq 0 \quad (4)$$

where

$$\omega_1 = \frac{-\alpha\xi + \xi\sqrt{\alpha^2 + 4\beta(1+\xi)}}{4(1+\xi)}\eta, \quad \omega_2 = \frac{\alpha\eta}{1+\xi} - \frac{(1+\xi-\eta)(-\alpha + \sqrt{\alpha^2 + 4\beta(1+\xi)})}{2(1+\xi)}$$

where α, β, η , and ξ are constants.

Meshless methods are a class of numerical methods that are used to simulate in essentially every field of science, mathematics, and computational biology [3-6]. It has been one of the hottest topics in computational mathematics in recent years, with an increasing number of scholars dedicating themselves to the study of meshfree methods, which have been suggested to solve various types of ODE and PDE. To solve PDE utilizing meshless methods with freely distributed collocations in the computational domain, and these collocation points participate to the approximation via assumed global or local basis functions. As contrary to most mesh-based methods, the spatial domain is represented by a set of nodes in meshless methods. As a result, there is no need for predetermined connectivity between the nodes. These methods solve the challenges of dimensionality. Meshless methods are efficient and produced better accuracy and can compute the solution in both regular and irregular computational domains. Meshless techniques based on radial basis functions have some limitations, the most significant of which is choosing the optimal shape-parameter value and dense ill-conditioned matrices. To avoid these weaknesses, researchers have introduced several techniques which makes these methods more efficient and accurate. These approaches have recently been tested in a variety of applications [7-18]. In this study, we have used the local differential quadrature method (LDQM) and the global meshless method of line (GMOL) for the numerical simulation of the generalized Burger's-Huxley eq. (1).

Methodologies

According to the proposed LDQM, the derivatives of $W(x, t)$ are approximated at the centers x_h by the neighborhood of

$$x_h, \{x_{h1}, x_{h2}, x_{h3}, \dots, x_{hn_h}\} \subset \{x_1, x_2, \dots, x_{N^n}\}, n_h \ll N^n, \text{ where } h = 1, 2, \dots, N^n$$

$$W^{(m)}(x_h) \approx \sum_{k=1}^{n_h} \lambda_k^{(m)} W(x_{hk}), \quad h = 1, 2, \dots, N \quad (5)$$

Substituting RBF $\psi\|x - x_p\|$ in eq. (5):

$$\psi^{(m)}(\|x_h - x_p\|) = \sum_{k=1}^{n_h} \lambda_{hk}^{(m)} \psi(\|x_{hk} - x_p\|), \quad p = h_1, h_2, \dots, hn_h \quad (6)$$

where for multiquadric (MQ) RBF, we have

$$\psi(\|x_{hk} - x_p\|) = \sqrt{1 + (c\|x_{hk} - x_p\|)^2}$$

Matrix form of eq. (6):

$$\underbrace{\begin{bmatrix} \psi_{h1}^{(m)}(x_h) \\ \psi_{h2}^{(m)}(x_h) \\ \vdots \\ \psi_{hn_h}^{(m)}(x_h) \end{bmatrix}}_{\boldsymbol{\psi}_{n_h}^{(m)}} = \underbrace{\begin{bmatrix} \psi_{h1}(x_{h1}) & \psi_{h2}(x_{h1}) & \cdots & \psi_{hn_h}(x_{h1}) \\ \psi_{h1}(x_{h2}) & \psi_{h2}(x_{h2}) & \cdots & \psi_{hn_h}(x_{h2}) \\ \vdots & \vdots & \ddots & \vdots \\ \psi_{h1}(x_{hn_h}) & \psi_{h2}(x_{hn_h}) & \cdots & \psi_{hn_h}(x_{hn_h}) \end{bmatrix}}_{\mathbf{A}_{n_h}} \underbrace{\begin{bmatrix} \lambda_{h1}^{(m)} \\ \lambda_{h2}^{(m)} \\ \vdots \\ \lambda_{hn_h}^{(m)} \end{bmatrix}}_{\boldsymbol{\lambda}_{n_h}^{(m)}} \quad (7)$$

where

$$\psi_p(x_k) = \psi(\|x_k - x_p\|), \quad p = h1, h2, \dots, hn_h$$

for each $k = i_1, h_2, \dots, hn_h$. The eq. (12) can be written:

$$\boldsymbol{\psi}_{n_h}^{(m)} = \mathbf{A}_{n_h} \boldsymbol{\lambda}_{n_h}^{(m)} \quad (8)$$

From eq. (8), we obtain:

$$\boldsymbol{\lambda}_{n_h}^{(m)} = \mathbf{A}_{n_h}^{-1} \boldsymbol{\psi}_{n_h}^{(m)} \quad (9)$$

eqs. (5) and (9) implies

$$W^{(m)}(x_h) = \left(\boldsymbol{\lambda}_{n_h}^{(m)} \right)^T \mathbf{W}_{n_h}$$

where

$$\mathbf{W}_{n_h} = \left[W(x_{h1}), W(x_{h2}), \dots, W(x_{hn_h}) \right]^T$$

According to the global meshless method of line, we approximate the function $W(x)$, which is denoted by $W(x)$:

$$W^{(N)}(x) = \sum_{k=1}^N \lambda_k \psi_k = \boldsymbol{\Phi}(x) \boldsymbol{\lambda} \quad (10)$$

where

$$\boldsymbol{\Phi}(x) = [\psi_1, \psi_2, \psi_3, \dots, \psi_N]^T, \quad \boldsymbol{\lambda} = [\lambda_1, \lambda_2, \lambda_3 \dots \lambda_N]$$

Let $W(x_k) = W_k$, then:

$$\mathbf{A} \boldsymbol{\lambda} = \mathbf{W} \quad (11)$$

where $\mathbf{W} = [W_1, W_2, W_3, \dots, W_N]^T$:

$$\mathbf{A} = \begin{bmatrix} \boldsymbol{\Phi}^T(x_1) \\ \boldsymbol{\Phi}^T(x_2) \\ \vdots \\ \boldsymbol{\Phi}^T(x_N) \end{bmatrix} = \begin{bmatrix} \psi_1(x_1) & \psi_2(x_1) & \cdots & \psi_N(x_1) \\ \psi_1(x_2) & \psi_2(x_2) & \cdots & \psi_N(x_2) \\ \vdots & \vdots & \ddots & \vdots \\ \psi_1(x_N) & \psi_2(x_N) & \cdots & \psi_N(x_N) \end{bmatrix} \quad (12)$$

From eqs. (10) and (11), we have:

$$W^N(x) = \Phi^T(x) \mathbf{A}^{-1} W = \mathbf{H}(x) W \quad (13)$$

where $\mathbf{H}(x) = \Phi^T(x) \mathbf{A}^{-1}$.

Implementing the aforementioned procedures, we approximate the space derivatives of the governing (1), which convert it to system of ODE. Next, we will utilize the classical Euler scheme to solve it. The global method of line is a standard meshless procedure which can be found in detail in [13, 14].

Numerical discussion

The proposed LDQM and GMOL are tested for applicability, accuracy, and efficiency to approximate the solution of model eq. (1). Throughout the paper, we have used MQ RBF with shape parameter value $c = 10$ (for LDQM) and $c = 1.1$ (for GMOL). The time step size $dt = 0.001$, spatial domain $[0, 1]$ and nodes $N = 10$ are utilized unless mentioned explicitly. For accuracy measurement, we used the following error norms:

$$\begin{aligned} \text{max-error} &= \max(|\widehat{W} - W|) \\ \text{RMS} &= \sqrt{\frac{\sum_{i=1}^N (\widehat{W}_i - W_i)^2}{N}} \end{aligned} \quad (14)$$

where W is the approximate solution and \widehat{W} is exact solution.

Test Problem 1. The proposed LDQM and GMOL are utilized to approximate the numerical results for Test Problem 1 and listed in tabs. 1 and 2 and figs. 1 and 2. In tab. 1, different values of final time, t , are used to compute the results whereas in tab. 1 various parameters values are considered. In viewed the tabulated results, very good agreement with the exact solution can be seen. In fig. 1, numerical solution for different time is visualized whereas in fig. 2, error is shown for both the methods. From these we can say that reasonable good accuracy have been obtained in both case but accuracy wise the GMOL is better in this case.

Table 1. Test Problem 1, numerical results for $\alpha = \beta = \zeta = 1, \eta = 0.001$

t	LDQM		GMOL	
	Max-error	RMS	Max-error	RMS
	$4.6891 \cdot 10^{-08}$	$3.2649 \cdot 10^{-08}$	$4.8147 \cdot 10^{-08}$	$3.3772 \cdot 10^{-08}$
	$4.6894 \cdot 10^{-08}$	$3.2651 \cdot 10^{-08}$	$4.8150 \cdot 10^{-08}$	$3.3775 \cdot 10^{-08}$
	$4.6894 \cdot 10^{-08}$	$3.2651 \cdot 10^{-08}$	$4.8152 \cdot 10^{-08}$	$3.3776 \cdot 10^{-08}$

Table 2. Test Problem 1, the max-error of the LDQM and the GMOL

Method	$\alpha = 0, \beta = 1, \zeta = 1, \eta = 0.001$		$\alpha = 0, \beta = 1, \zeta = 2, \eta = 0.001$		$\alpha = 0, \beta = 1, \zeta = 3, \eta = 0.001$	
	$t = 1$	$t = 10$	$t = 1$	$t = 10$	$t = 1$	$t = 10$
LDQM	$6.2506 \cdot 10^{-08}$	$6.2508 \cdot 10^{-08}$	$2.7943 \cdot 10^{-06}$	$2.7817 \cdot 10^{-06}$	$9.9144 \cdot 10^{-06}$	$9.8247 \cdot 10^{-06}$
GMOL	$6.3763 \cdot 10^{-08}$	$6.3770 \cdot 10^{-08}$	$2.8505 \cdot 10^{-06}$	$2.8382 \cdot 10^{-06}$	$1.0114 \cdot 10^{-05}$	$1.0025 \cdot 10^{-05}$

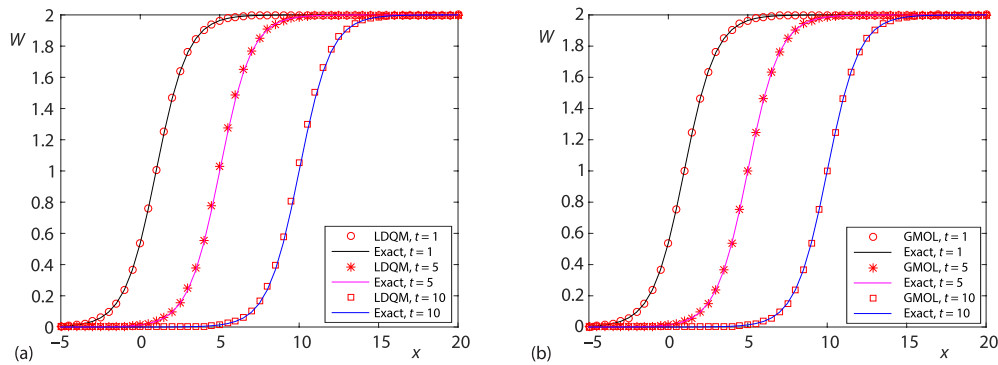


Figure 1. Test Problem 1, numerical solution for $\alpha = \beta = \zeta = 1, \eta = 2$; (a) the LDQM and (b) the GMOL

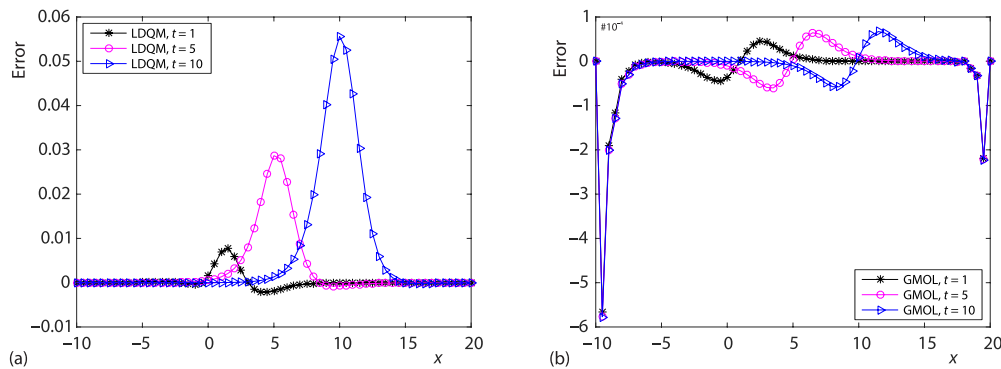


Figure 2. Test Problem 1, plot of error for $\alpha = \beta = \zeta = 1, \eta = 2$; (a) the LDQM and (b) the GMOL

Conclusion

In the current research work, we have utilized two methods, the local differential quadrature and the global method of line which are based on radial basis functions, as a modern powerful numerical methods to investigate the generalized Burger's-Huxley equation. First, both the schemes are employed to discretize the problem in the space direction and secondly, Euler method is used for time derivative. The proposed algorithms approximated the solution with good accuracy and in light of these analyses, we suggest that both algorithms can be implemented to such types non-linear PDE models which appear in physical problems.

Acknowledgment

Taif University Researchers Supporting Project No. (TURSP-2020/154), Taif University, Taif, Saudi Arabia.

References

- [1] Satsuma, J., et al., *Topics in Soliton Theory and Exactly Solvable Non-linear Equations*, World Scientific, Singapore, Singapore 1987
- [2] Wang, X. Y., et al., Solitary Wave Solutions of the Generalized Burger's-Huxley equation, *Journal Phys. A: Math. Gen.*, 23 (1990), 3, pp. 271-274
- [3] Wang, F., et al., Gaussian Radial Basis Functions Method for Linear and Non-Linear Convection-Diffusion Models in Physical Phenomena, *Open Phys.*, 19 (2021), 1, pp. 69-76

- [4] Hussain, Z., et al., Extension of Optimal Homotopy Asymptotic Method with Use of Daftardar-Jeffery Polynomials to Hirota-Satsuma Coupled System of Korteweg de Vries Equations, *Open Phys.*, 18 (2020), 1, pp. 916-924
- [5] Ahmad, I., et al., Solution of Multi-Term Time-Fractional PDE Models Arising in Mathematical Biology and Physics by Local Meshless Method, *Symmetry*, 12 (2020), 7, 1195
- [6] Ahmad, I., et al., Numerical Simulation of PDE by Local Meshless Differential Quadrature Collocation Method, *Symmetry*, 11 (2019), 3, 394
- [7] Thounthong, P., et al., Symmetric Radial Basis Function Method for Simulation of Elliptic Partial Differential Equations, *Mathematics*, 6 (2018), 12, 327
- [8] Wang, F., et al., A Novel Meshfree Strategy for a Viscous Wave Equation with Variable Coefficients, *Front. Phys.*, 9 (2021), 359
- [9] Li, J. F., et al., Numerical Solution of Two-Term Time-Fractional PDE Models Arising in Mathematical Physics Using Local Meshless Method, *Open Phys.*, 18 (2021), 1, pp. 1063-1072
- [10] Khan, M. N., et al. Numerical Solution of Time-Fractional Coupled Korteweg-de Vries and Klein-Gordon Equations by Local Meshless Method, *Pramana*, 95 (2021), 1, pp. 1-13
- [11] Srivastava H. M., et al., Numerical Simulation of 3-D Fractional-Order Convection-Diffusion PDE by a Local Meshless Method, *Thermal Science*, 25 (2020), 1A, pp. 347-358
- [12] Ahmad, I., et al., Application of local Meshless Method for the Solution of Two Term Time Fractional-Order Multi-Dimensional PDE Arising in Heat and Mass Transfer, *Thermal Science*, 24 (2020), 1, pp. 95-105
- [13] Shen, Q., A Meshless Method of Lines for the Numerical Solution of KdV Equation Using Radial Basis Functions, *Eng. Anal. Bound. Elem.*, 33 (2009), 10, pp. 1171-1180
- [14] Haq, S., et al., Meshless Method of Lines for the Numerical Solution of Generalized Kuramoto-Sivashinsky Equation, *Appl. Math. Comput.*, 217 (2010), 6, pp. 2404-2413
- [15] Ulutas, E., et al., Bright, Dark, and Singular Optical Soliton Solutions for Perturbed Gerdjikov-Ivanov Equation, *Thermal Science*, 25 (2021), Special Issue 2, pp. S151-S156
- [16] Ulutas, E., et al., Exact Solutions of Stochastic KdV Equation with Conformable Derivatives in white Noise Environment, *Thermal Science*, 25 (2021), Special Issue 2, pp. S143-S149
- [17] Yildirim, E. N., et al., Reproducing Kernel Functions and Homogenizing Transforms, *Thermal Science*, 25 (2021), Special Issue 2, pp. S9-S18
- [18] Abdelrahman, M. A. E., et al., Exact Solutions of the Cubic Boussinesq and the Coupled Higgs Systems, *Thermal Science*, 24 (2020), Suppl. 1, pp. S333-S342